2020

Quantum cascade laser-based reflectance spectroscopy: a robust approach for the classification of plastic type

Anna P.M. Michel

Alexandra E. Morrison

Beckett C. Colson

William A. Pardis

Helen K. White

Research Article Vol. 28, No. 12 / 8 June 2020 / Optics Express 17741
Optics EXPRESS

Quantum cascade laser-based reflectance spectroscopy: a robust approach for the classification of plastic type

ANNA P. M. MICHEL,[1,*] ALEXANDRA E. MORRISON,[1] BECKETT C. COLSON,[1,2] WILLIAM A. PARDIS,[1] XAVIER A. MOYA,[3] CHARLES C. HARB,[3] AND HELEN K. WHITE[4]

[1]*Department of Applied Ocean Physics and Engineering, Woods Hole Oceanographic Institution, 266 Woods Hole Road, Woods Hole, Massachusetts 02543, USA*
[2]*Department of Mechanical Engineering, Massachusetts Institute of Technology, 77 Massachusetts Avenue, Cambridge, Massachusetts 02139, USA*
[3]*RingIR Inc. 609 Broadway Boulevard NE, Albuquerque, New Mexico 87102, USA*
[4]*Departments of Chemistry and Environmental Studies, Haverford College, Haverford, Pennsylvania 19041, USA*
[*]*amichel@whoi.edu*

Abstract: The identification of plastic type is important for environmental applications ranging from recycling to understanding the fate of plastics in marine, atmospheric, and terrestrial environments. Infrared reflectance spectroscopy is a powerful approach for plastics identification, requiring only optical access to a sample. The use of visible and near-infrared wavelengths for plastics identification are limiting as dark colored plastics absorb at these wavelengths, producing no reflectance spectra. The use of mid-infrared wavelengths instead enables dark plastics to be identified. Here we demonstrate the capability to utilize a pulsed, widely-tunable (5.59 - 7.41 μm) mid-infrared quantum cascade laser, as the source for reflectance spectroscopy, for the rapid and robust identification of plastics. Through the application of linear discriminant analysis to the resulting spectral data set, we demonstrate that we can correctly classify five plastic types: polyethylene terephthalate (PET), high density polyethylene (HDPE), low density polyethylene (LDPE), polypropylene (PP), and polystyrene (PS), with a 97% accuracy rate.

1. Introduction

The robust and rapid identification of plastic type is needed for environmental applications ranging from recycling facilities to understanding sources and sinks of plastics in the environment. For example, to understand plastic fate and transport in the environment, it is important to be able to robustly classify plastics found in locations ranging from land to the deep sea. Although hundreds of types of plastics exist with added complexity due to fillers, additives, and colorants, plastics are often identified by their recycling codes: #1 polyethylene terephthalate (PET), #2 high density polyethylene (HDPE), #3 polyvinyl chloride (PVC), #4 low density polyethylene (LDPE), #5 polypropylene (PP), #6 polystyrene (PS), and #7 other plastics.

Optical approaches for plastics classification allow samples to be identified in both stand-off configurations and in a non-destructive manner, with no damage to a sample. A range of optical approaches have been utilized for plastics classification [1], including attenuated total reflectance - Fourier transform infrared spectroscopy (ATR-FTIR) [2], laser induced breakdown spectroscopy (LIBS) (e.g. [3–5]), near-infrared reflectance spectroscopy (NIR) [6], and Raman spectroscopy [7]. Hybrid approaches, such as combining Raman and LIBS techniques, have also been applied to plastics identification [8]. There are challenges to some of these approaches; for example, NIR spectroscopy is limited for plastics identification, as the wavelengths cannot be used to identify

#393231 https://doi.org/10.1364/OE.393231
Journal © 2020 Received 19 Mar 2020; revised 15 May 2020; accepted 16 May 2020; published 28 May 2020

Optics EXPRESS

black or dark (e.g. dark grey) plastics due to their low reflectance in the NIR spectral range. In the NIR region, other materials such as carbon black and soot both absorb completely [9]. For polymer sorting, Fourier transform infrared (FTIR) spectroscopy is typically too slow [9]. To address these limitations, it is important that a wide range of optical approaches for plastic identification be explored.

Mid-infrared (MIR) wavelengths are of particular interest for plastics identification, in particular, MIR quantum cascade lasers (QCLs), which are compact and can be made both high power and widely tunable. QCLs have been demonstrated to have applications ranging from trace gas detection (e.g. [10–12]) to explosives detection [13] to medically relevant compounds such as glucose, lactate and triglycerides [14–16]. The ability to be widely tunable makes them a viable source for covering a large spectral range and for measuring broadband absorbers. The compact design of the QCL and its ability to be used in a stand-off/remote operation make them a viable source for implementation in small, field portable sensors. Specular reflectance spectroscopy is a powerful and simple approach, only requiring optical access to a sample. Such an approach reduces the possibility of sample cross-contamination. For example, other MIR wavelength techniques such as FTIR and ATR-FTIR (e.g. [17–19]), require physical contact with the sample, which could result in cross-contamination if the sample, residues, or biofilms stick to the contacting crystal. Here we demonstrate the coupling of QCL-based reflectance spectroscopy with a classifier technique, linear discriminant analysis, for the accurate identification of plastic samples.

2. Materials and methods

2.1. Plastic samples

Macroplastic samples from newly purchased consumer, laboratory, and hardware products with plastic type identified based on imprinted recycling code labels were selected (Table 1). Thirty samples of each of five types of plastics, PET, HDPE, LDPE, PP, and PS, for a total of 150 samples were selected (physical sample descriptions detailed in Appendix A, Table 6). The plastic samples included a range of color, opaqueness, and thickness. Thin film plastics were not selected due to the challenge they present with interference fringes from back-surface reflection; thus, all plastics selected were at least 0.13 mm thick. All samples were rinsed with deionized water and cut to a size of approximately 2 cm x 2 cm before analysis.

2.2. Quantum cascade laser reflectance

2.2.1. Optical set-up

A widely tunable (5.59 - 7.41 μm / 1789.87-1350.07 cm^{-1}) pulsed external cavity QCL (maximum average power 28 mW; Daylight Solutions Inc.) was selected based on its wavelength coverage of the key spectral peaks, identified previously by ATR-FTIR, of the five targeted plastics [2,18]. The QCL was pulsed at a 5.0% duty cycle, 100 kHz pulse repetition rate, with a 500 ns pulse width. A 45 degree fixed angle specular reflection accessory (Pike Technologies, 45Spec Accessory, 011-4500) with a 10 mm mask was utilized for sample analysis; samples were laid across the opening of the mask (Fig. 1). The laser beam has an ~2.5 mm beam width at the $1/e^2$ point. As a result, the laser beam diameter was less than the plastic area revealed through the mask, and the laser beam only interacted with the plastic sample and did not touch the mask. A gold mirror followed by a weight was placed on top of each sample to maintain or improve sample flatness as the plastic samples were often irregular in thickness. A 9 μm thermoelectrically-cooled mercury-cadmium-telluride (MCT) detector (Vigo - PCI-2TE-9) coupled to a pre-amplifier was used for collection of specularly reflected light. Two CaF_2 holographic wire grid polarizers (Thorlabs, WP25H-C) were placed in the beam path to reduce the amount of light received by the detector to avoid saturation. A lock-in amplifier (Zurich Instruments - HF2LI) was used

Optics EXPRESS

Table 1. Thirty consumer plastic samples from five different types of plastics were selected[a].

Recycling Code	Plastic Type	Sample Colors	Sample Opaqueness	Thickness Range (mm)
1	Polyethylene terephthalate (PET)	Clear, red, blue, green	Clear, opaque	0.13–1.62
2	High density polyethylene (HDPE)	White, green, black, orange, brown, clear, turquoise	Semi-opaque, opaque	0.42 - 2.02
4	Low density polyethylene (LDPE)	Clear, white, red, blue, yellow	Clear, semi-opaque, opaque	0.59–12.74
5	Polypropylene (PP)	Black, clear, white, blue	Clear, semi-opaque, opaque	0.42–1.36
6	Polystyrene (PS)	White, purple, clear, black	Clear, semi-opaque, opaque	0.20–11.57

[a]The samples selected included a range of colors, opaqueness, and thickness.

for signal collection from the detector and data were recorded using MATLAB (R2018a). A background measurement using the gold mirror was collected prior to the measurement of every fifth plastic sample to monitor any changes in laser output power. For each mirror or plastic sample measurement, the QCL was scanned across its full tuning range 5 times. Each output reflection spectrum recorded was thus the average of 5 spectra. A single scan took approximately 5 seconds; therefore, the total time for the 5 spectra was 25 seconds. Each plastic sample was analyzed in triplicate, moving the sample between each measurement; resulting in 450 total spectra (three reflection spectra of each of the 150 plastic samples).

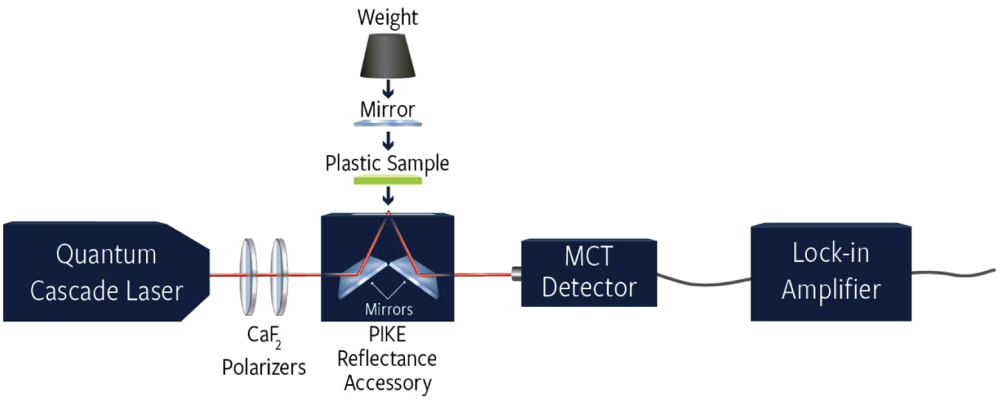

Fig. 1. Optical layout. A widely-tunable quantum cascade laser was used as the source. Samples were placed onto a PIKE reflectance accessory (45°) along with a mirror and a weighted block. Two polarizers were used to limit the amount of light reaching the detector to avoid saturation. Specularly reflected light was collected by a detector and the signals recorded using a lock-in amplifier and a laptop running MATLAB (R2018a).

Optics EXPRESS

2.2.2. Data processing

The QCL spectrum of each plastic sample $I(\nu)$ was normalized by dividing by the background mirror spectrum $I_0(\nu)$, and then was converted to the normalized specular absorbance spectrum $A(\nu) = -\log(I(\nu)/I_0(\nu))$. This spectrum was then converted to its imaginary analytic signal using the Hilbert transform function in MATLAB (R2018a). The Hilbert transform was utilized as an alternative to the Kramers-Kronig [20].

The resulting spectrum was smoothed (moving average of 150) and then the 1697-1550 cm^{-1} region was removed from each spectrum due to a lack of identifying spectral features for plastics in this region. The removal of this region enabled a reduction in size of the spectral dataset and limited excess noise from entering the classification model.

2.2.3. Classification model

Linear discriminant analysis, a technique used to reduce the number of variables in a dataset, can be used as a classifier for modeling differences of groups. Linear discriminant analysis, implemented using the MATLAB Machine Learning toolbox, was utilized to develop a classification model. The dataset of 450 total spectra was split into a training set (two-thirds of the samples) and a holdout test set (remaining third of the samples). The holdout test set was chosen via a stratified random sample to ensure that the prediction accuracy on each class was equally weighted in the test accuracy. In order to capture any variance in the data, the training and test sets were randomly resampled ten times and the analysis was repeated as separate trials. The final reported test accuracy and confusion matrix results are the average of the ten repeated trials.

Linear discriminant analysis was then applied to only the HDPE and LDPE spectra to confirm that these plastic types could be classified correctly based on small differences in their two spectral peaks in the 1477-1458 cm^{-1} region. To confirm this, only HDPE and LDPE were used in a second classification model following the same approach as when all of the plastics were used. Two approaches were used 1) using the full spectral region (minus the omitted portion as described previously) and 2) using only the 1477-1458 cm^{-1} region of the HDPE and LDPE samples.

2.3. Attenuated total reflectance-Fourier transform infrared (ATR-FTIR) spectroscopy

Five representative samples were selected for ATR-FTIR analysis (PET02, PP22, HDPE28, LDPE17, and PS05, detailed in Appendix A, Table 6) to determine peak position for comparison with the QCL-reflectance data. ATR-FTIR was performed on these five samples in triplicate. These measurements were made using an Agilent Technologies Cary 630 FTIR spectrometer coupled to a D-ATR diamond crystal accessory with a single reflection sensor and a sample press. Absorbance spectra were collected using 32 scans at a 2 cm^{-1} resolution measuring between 4000 - 650 cm^{-1}. A background atmospheric spectrum was subtracted from all sample spectra.

2.4. Fourier transform infrared (FTIR) spectroscopy

A Fourier transform infrared spectrometer (Bruker Vertex 80) was utilized in reflectance mode using the 45 degree fixed angle specular reflection accessory (Pike Technologies, 45Spec Accessory, 011-4500) in the sample compartment. A broadband mid-infrared globar along with a KBr beamsplitter, and a liquid nitrogen-cooled MCT detector with a ZnSe window that covers the 12,000 cm^{-1} to 600 cm^{-1} region. Each plastic was placed on top of the reflection accessory and a gold mirror was used to calculate a background spectrum. Spectra were collected using 32 scans with a spectral resolution of 2 cm^{-1} measuring between 1300 - 1800 cm^{-1}. The Hilbert transform was applied using MATLAB (R2018a), and spectra were smoothed with a moving average of 10.

Optics EXPRESS

3. Results and discussion

3.1. QCL reflectance spectra reveal distinct features for different plastic types

The QCL reflectance spectra showed clear peaks corresponding to known distinct features for all five of the plastics, with similarities in peak location for HDPE and LDPE (Fig. 2). Significant spectra-to-spectra variability among replicate runs of the same plastic sample existed, which we attribute to changes in reflection due to how the sample was placed on the reflection accessory, as each sample was moved between replicates. However, the key spectral features did not vary in location. Variability existed between different samples of the same type, which we additionally attribute to variations in plastic formulation (e.g. stabilizers, fillers, colorants, and additives) and physical variability of the samples (e.g. differences in smoothness, shininess, opaqueness, and color) (Fig. 3). Interference fringe patterns were observed in some spectra, which we hypothesize is due to refractive index differences with these plastics. Despite the differences between spectra of the same plastic type, the distinct spectral features identified for each type of plastic appeared in 95% of all spectra. Only in 21 measurements out of the 450 measurements were spectral features not clearly identifiable.

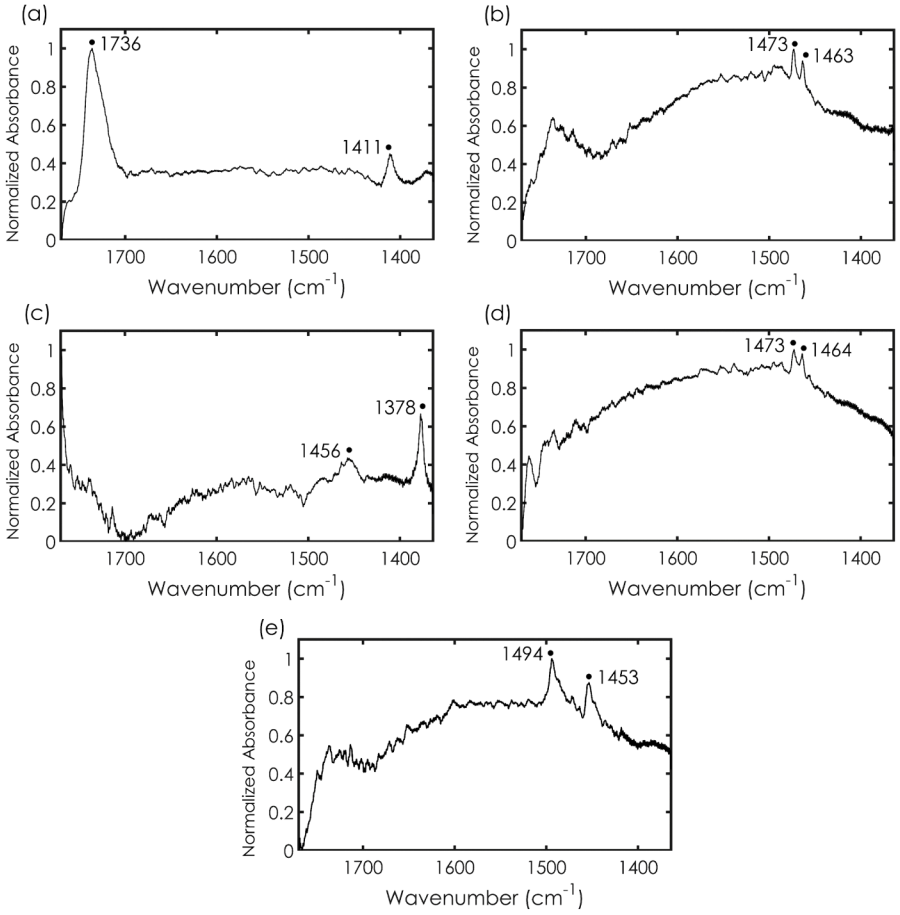

Fig. 2. QCL representative spectra (smoothed with a moving average of 150 data points and shown normalized on a 0 to 1 scale) of (a) PET (sample PET02) (b) HDPE (sample HDPE28) (c) PP (sample PP22) (d) LDPE (sample LDPE17) (e) PS (sample PS05). Peaks corresponding to plastic type are labeled. Peaks are shown in cm^{-1}.

Optics EXPRESS

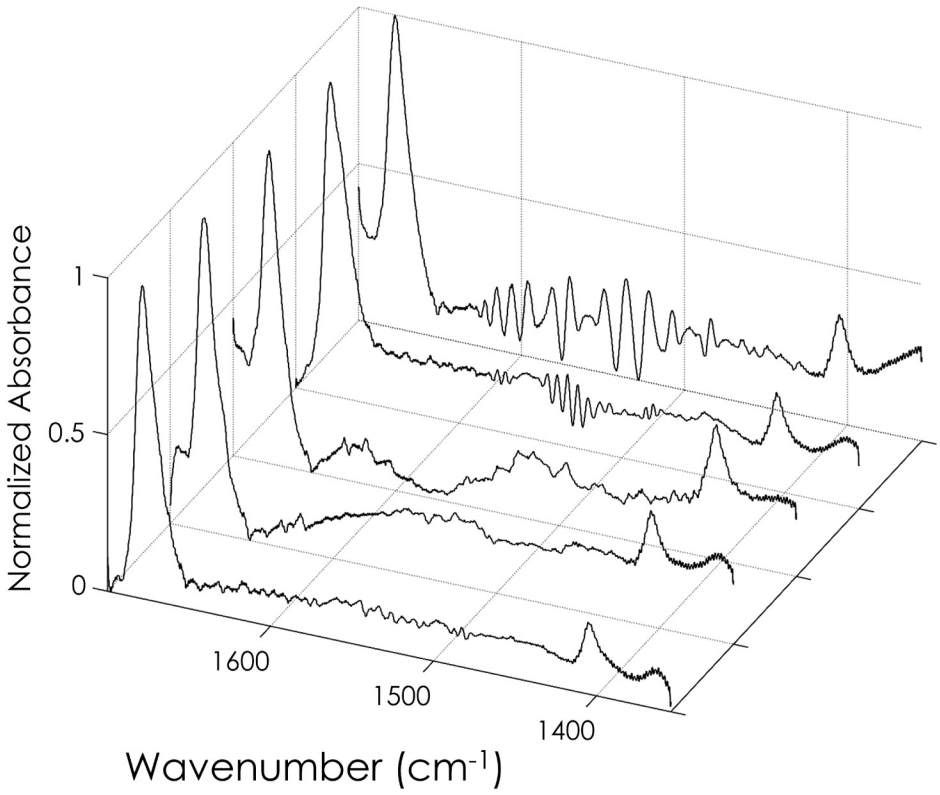

Fig. 3. Variability between spectra of 5 different PET samples (shown normalized on a 0 to 1 scale). (Front to back: PET19, PET01, PET13, PET21, PET07). The characteristic PET peaks at 1736 cm^{-1} and 1411 cm^{-1} remain in each sample, and increased variability in the 1697-1550 cm^{-1} region is not indicative of plastic type and not used for analysis.

To examine the influence of color on spectra, we compared a black HDPE sample and a white HDPE sample analyzed using the QCL reflectance setup. The spectra show clearly visible peaks at 1473 cm^{-1} and 1463 cm^{-1} in both spectra (Fig. 4). This ability to analyze dark plastic samples is a key advantage of the utilization of mid-infrared wavelengths instead of near-infrared for plastics identification.

3.2. Comparisons of peak locations and ease of analysis for QCL, ATR-FTIR and FTIR

The spectral peaks present in the QCL reflectance spectra were compared to ATR-FTIR spectra reported in the literature as well as spectra taken in the laboratory using both ATR-FTIR (Fig. 5) and FTIR-reflectance spectroscopy (Fig. 6, Table 2). Limitations in these techniques must be noted as ATR-FTIR requires that the sample be physically in contact for the measurement and our FTIR measurements required the use of a liquid nitrogen-cooled detector. For ATR-FTIR, the peak locations reported in the literature [2] aligned with those we measured (Fig. 5; Table 2). ATR-FTIR is routinely used for plastics analysis including microplastics analysis. Differences in peak location however were observed between the ATR-FTIR measurements when compared to those seen in the FTIR-reflectance and QCL-reflectance data, both of which were in agreement with each other. At the longer wavelengths measured, ATR spectral peaks are often shifted towards lower frequencies (shift in peak position) when compared to transmission or reflectance

Optics EXPRESS

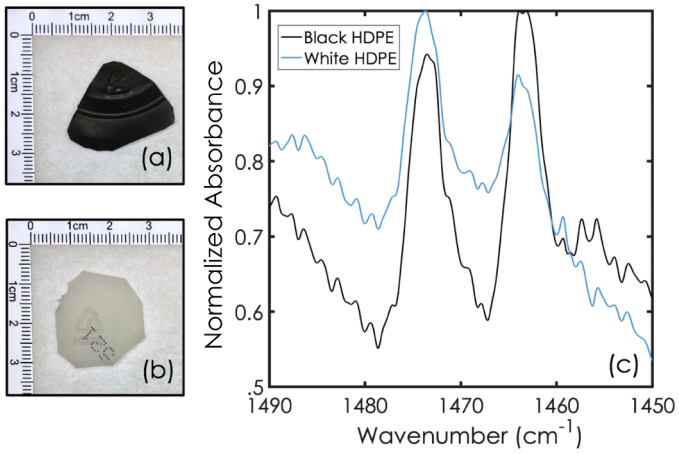

Fig. 4. Comparison of spectra of a black and a white HDPE plastic sample. (a) Photo of a black HDPE sample. (b) Photo of a white HDPE sample. (c) HDPE characteristic spectral peaks at 1473 cm^{-1} and 1463 cm^{-1}. Spectra smoothed by 150 point moving average and shown normalized on a 0 to 1 scale. Black spectrum = black HDPE sample. Blue spectrum = white HDPE sample.

spectra [21,22]. Since plastics are routinely identified spectrally in the infrared region by their characteristic peaks, it is important to recognize these shifts.

Table 2. Spectral peaks[a]

Plastic Type	ATR-FTIR Peak (cm^{-1}) (previously reported)[b]	ATR-FTIR Peak (cm^{-1}) Laboratory	Reflectance Peak - FTIR (cm^{-1})	Reflectance Peak QCL (cm^{-1})
PET	1713 C = O stretch	1712	1736	1736
	1408 Aromatic Ring Stretch	1408	1411	1411
HDPE	1472 CH_3 Bend	1473	1473	1473
	1462 CH_2 Bend	1463	1463	1463
LDPE	1467 CH_2 Bend	1472	1473	1473
	1462 CH_2 Bend	1463	1463	1464
PP	1455 CH_2 Bend	1456	1458	1456
	1377 CH_3 Bend	1375	1377	1378
PS	1492 Aromatic Ring Stretch	1492	1494	1494
	1451 CH_2 Bend	1451	1453	1453

[a]Peaks shown have been previously reported for ATR-FTIR and were measured in the laboratory by ATR-FTIR, FTIR in reflectance mode, and using the QCL reflectance setup.
[b][2,23]

3.3. *Plastic-type identification using QCL reflectance spectroscopy*

The classification model using linear discriminant analysis resulted in a 97% correct identification rate for the 150 samples analyzed. The variability between spectra for the same plastic type is hypothesized as the cause of some misidentifications. All PET samples were correctly identified (Table 3), due to the strong spectral feature at 1736 cm^{-1}. For each of the other four plastic types, the model was also highly successful, resulting in at most 9 plastic samples being misidentified during a single model run, with most misclassifications occurring between HDPE and LDPE. For

Optics EXPRESS

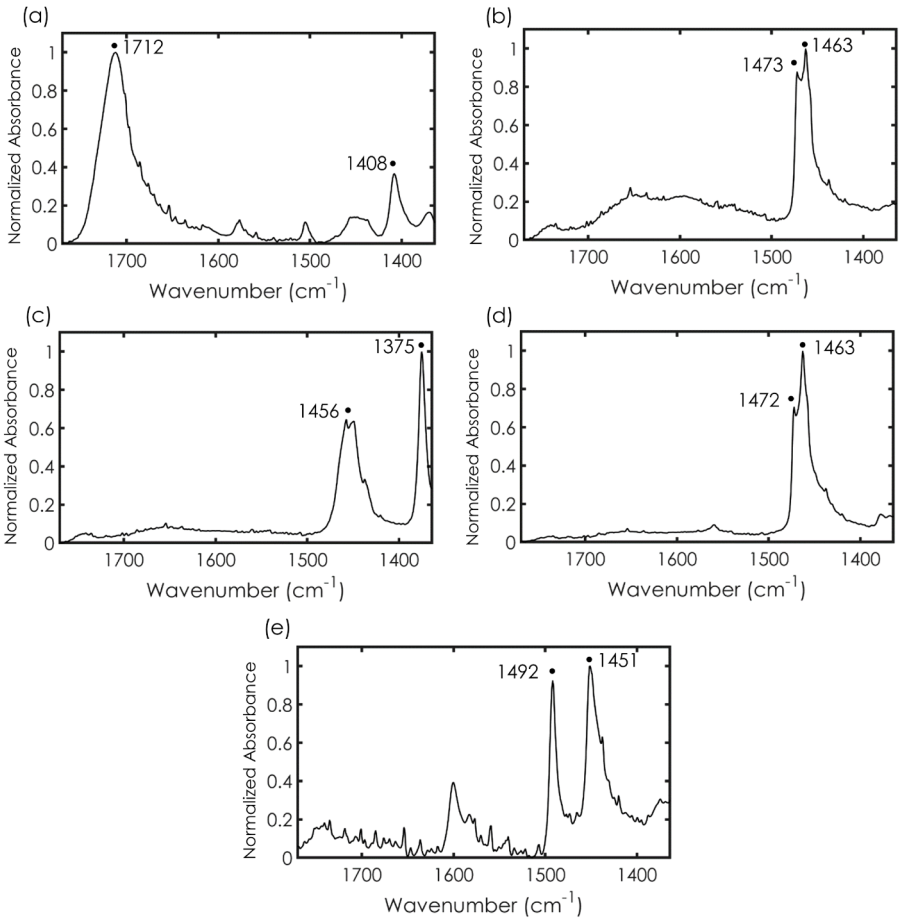

Fig. 5. ATR-FTIR representative spectra (shown normalized on a 0 to 1 scale) of (a) PET (sample PET02) (b) HDPE (sample HDPE28) (c) PP (sample PP22) (d) LDPE (sample LDPE17) (e) PS (sample PS05). Characteristic peaks corresponding to each plastic type are labeled. Peaks are shown in cm^{-1}.

example, during one model run, 6 HDPE samples were incorrectly classified as LDPE. HDPE and LDPE both have a spectral peak at 1463 cm^{-1} and a closely spaced second peak at 1473 cm^{-1} and 1472 cm^{-1} for HDPE and LDPE, respectively. To confirm that the slight peak difference allows for the discrimination of HDPE and LDPE, linear discriminant analysis was then run on only HDPE and LDPE. When the full spectral region (minus the chopped portion as described previously) was included, the success rate for identification between HDPE and LDPE was 88 +/- 4% (Table 4). When only the peak region (1477 - 1458 cm^{-1}) was utilized, the success rate increased to 97 +/- 3% (Table 5). Therefore, this suggests that the small difference in the HDPE and LDPE peaks allows for the discrimination to take place.

Optics EXPRESS

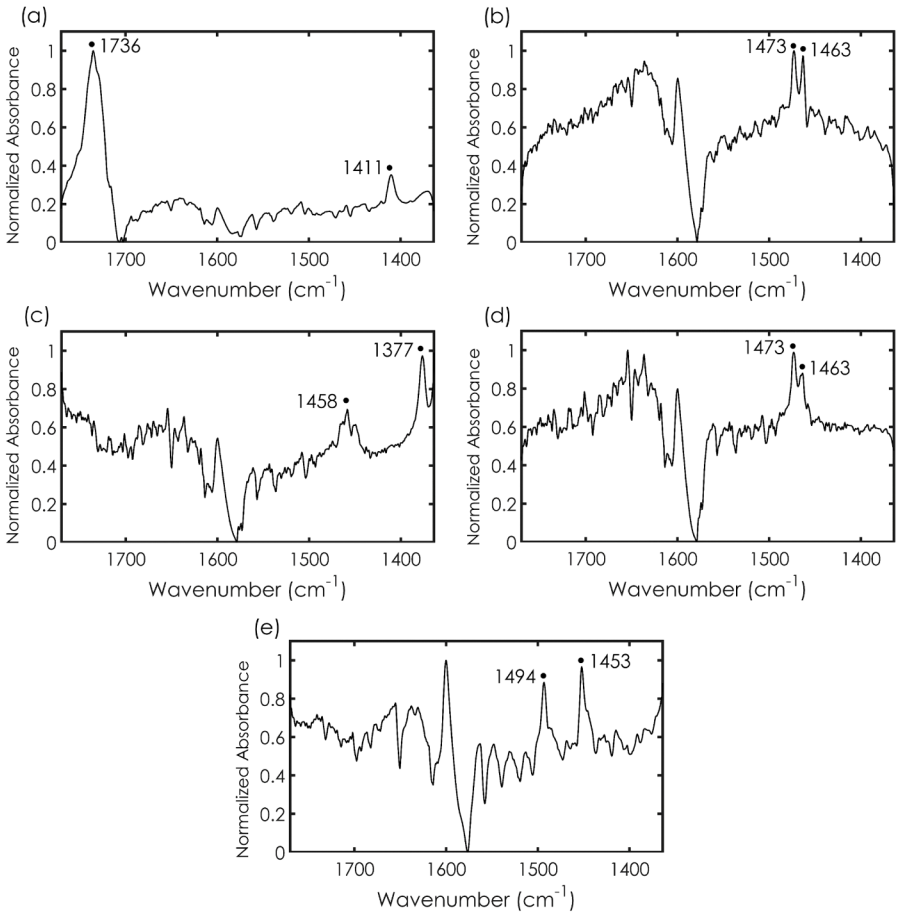

Fig. 6. Reflectance FTIR representative spectra (smoothed with a moving average of 10 data points and shown normalized) of (a) PET (sample PET02) (b) HDPE (sample HDPE28) (c) PP (sample PP22) (d) LDPE (sample LDPE17) (e) PS (sample PS05). Characteristic peaks corresponding to plastic type are labeled. Peaks are shown in cm^{-1}.

Table 3. Confusion matrix of linear discriminant analysis for the five plastics. Values on the diagonal (shaded and bolded) are correctly identified samples[a].

		Prediction				
		PET	**HDPE**	**LDPE**	**PP**	**PS**
Truth	**PET**	**30 ± 0**	0 ± 0	0 ± 0	0 ± 0	0 ± 0
	HDPE	0 ± 0	**28 ± 2**	2 ± 2	1 ± 1	0 ± 0
	LDPE	0 ± 0	1 ± 1	**29 ± 1**	0 ± 1	0 ± 0
	PP	0 ± 1	0 ± 1	0 ± 0	**29 ± 1**	0 ± 1
	PS	0 ± 0	0 ± 1	0 ± 0	0 ± 1	**29 ± 1**

[a]Values are the average and standard deviation of 10 repeated random splits of the data using test sets containing 30 measurements of each plastic type.

Optics EXPRESS

Table 4. Confusion matrix of linear discriminant analysis for HDPE and LDPE using full spectral region[a].

		Prediction	
		HDPE	LDPE
Truth	HDPE	**24 ± 3**	6 ± 3
	LDPE	2 ± 2	**28 ± 2**

[a]Values are the average and standard deviation of 10 replicates using test sets containing 30 measurements of each plastic type. Values on the diagonal (shaded and bolded) are correctly identified samples.

Table 5. Confusion matrix of linear discriminant analysis for HDPE and LDPE using the spectral region covering the peaks only (1477-1458 cm^{-1})[a].

		Prediction	
		HDPE	LDPE
Truth	HDPE	**29 ± 2**	2 ± 2
	LDPE	1 ± 1	**30 ± 1**

[a]Values are the average and standard deviation of 10 replicates using test sets containing 30 measurements of each plastic type. Values on the diagonal (shaded and bolded) are correctly identified samples.

4. Conclusion

QCL-based MIR reflectance spectroscopy coupled to a classification model using linear discriminant analysis was demonstrated to be a successful approach for rapid and robust identification of plastic type with a 97% correct identification rate. Each set of five spectra taken took only 25 seconds to acquire. In future set-ups, this could be reduced to one spectrum, resulting in a very rapid 5-second analysis time. While five different types of plastics were selected that had strong spectral features in the 5.59 to 7.41 μm region, other plastics, such as polyvinylchloride (PVC), were not included in this study due to the lack of strong spectral features in this region. However, due to the ability to design and fabricate QCLs at specific wavelengths, other plastics should also be identifiable using this same approach by selecting a QCL with the appropriate wavelength region. The use of widely-tunable QCLs (e.g. [24]), multiple QCLs or QCL arrays [25] would allow a broader range of plastic types to be distinguishable. QCL beam diameters are typically on the order of ~3mm in diameter [26] but can be focused down to reduce the beam to less than 300 μm (e.g. [27,28]), and some calculations point to beam diameters achieved as small as ~20 μm [26]. Although macroplastic samples were utilized here, the use of a smaller diameter beam would make it a viable approach for the analysis of smaller (<100 μm) plastic samples including microplastic (<5 mm) samples.

QCLs are tiny sources that can be designed to operate at mid-infrared wavelengths and at the same time can be made widely tunable. Incorporating a QCL into a small sensor, that does not require physical contact with the plastic sample, could have broad applications for the identification of plastic for recycling and environmental applications. If an environmental application was sought, future studies would be needed to examine plastic samples collected

Optics EXPRESS

from the environment, which have been chemically and physically weathered by environmental processes. This weathering, which could occur in both terrestrial and aqueous locations, has the potential to alter spectral peaks [29]. Other characteristics of samples found in the environment (e.g. wetness of sample, presence of water or fluids in a sample, presence of thin plastic or paper labels, curvature of surfaces) may introduce additional classification issues. Further laboratory studies would also be needed to fully understand these impacts and to design methodologies that allow for correct identification. The samples used in this study were newly acquired plastic samples and offer an important first-step in presenting the ability to use a QCL to identify plastic type.

Optics EXPRESS

Appendix A

Table 6. Sample name, recycling codes, plastic type, color, opaqueness, and thickness for each consumer plastic sample selected for this study.

Name	Recycling Code	Type	Color	Opaqueness	Thickness (mm)
PET01	1	PET	clear	clear	0.34
PET02	1	PET	red	opaque	0.56
PET03	1	PET	blue	clear	0.73
PET04	1	PET	bright blue	opaque	0.64
PET05	1	PET	clear	clear	0.40
PET06	1	PET	green	opaque	0.38
PET07	1	PET	clear	clear	0.33
PET08	1	PET	clear	clear	0.51
PET09	1	PET	clear	clear	0.14
PET10	1	PET	clear	clear	0.63
PET11	1	PET	clear	clear	0.32
PET12	1	PET	clear	clear	0.24
PET13	1	PET	clear	clear	0.32
PET14	1	PET	clear	clear	0.31
PET15	1	PET	clear	clear	0.58
PET16	1	PET	clear	clear	0.13
PET17	1	PET	clear	clear	0.25
PET18	1	PET	clear	clear	0.27
PET19	1	PET	clear	clear	0.23
PET20	1	PET	green	clear	0.48
PET21	1	PET	clear	clear	0.28
PET22	1	PET	clear	clear	0.29
PET23	1	PET	clear	clear	0.22
PET24	1	PET	clear	clear	0.99
PET25	1	PET	clear	clear	0.29
PET26	1	PET	clear	clear	1.62
PET27	1	PET	clear	clear	0.25
PET28	1	PET	clear	clear	0.38
PET29	1	PET	clear	clear	0.54
PET30	1	PET	clear	clear	0.36
HDPE01	2	HDPE	white	semi-opaque	0.71
HDPE02	2	HDPE	white	opaque	1.18
HDPE03	2	HDPE	white	opaque	0.66
HDPE04	2	HDPE	white	opaque	0.59
HDPE05	2	HDPE	green	opaque	1.82
HDPE06	2	HDPE	white	semi-opaque	0.95
HDPE07	2	HDPE	white	semi-opaque	1.28
HDPE08	2	HDPE	white	opaque	0.53

Optics EXPRESS

Name	Recycling Code	Type	Color	Opaqueness	Thickness (mm)
HDPE09	2	HDPE	white	opaque	1.49
HDPE10	2	HDPE	black	opaque	1.73
HDPE11	2	HDPE	white	opaque	0.51
HDPE12	2	HDPE	white	opaque	1.58
HDPE13	2	HDPE	white	semi-opaque	1.12
HDPE14	2	HDPE	white	semi-opaque	2.02
HDPE15	2	HDPE	orange	opaque	0.86
HDPE16	2	HDPE	white	semi-opaque	1.47
HDPE17	2	HDPE	white	semi-opaque	0.72
HDPE18	2	HDPE	white	semi-opaque	0.75
HDPE19	2	HDPE	white	opaque	1.89
HDPE20	2	HDPE	white	opaque	0.45
HDPE21	2	HDPE	brown	opaque	1.50
HDPE22	2	HDPE	white	opaque	1.34
HDPE23	2	HDPE	white	semi-opaque	0.68
HDPE24	2	HDPE	clear	semi-opaque	0.87
HDPE25	2	HDPE	clear	semi-opaque	0.42
HDPE26	2	HDPE	turquoise	opaque	0.51
HDPE27	2	HDPE	white	semi-opaque	0.44
HDPE28	2	HDPE	white	semi-opaque	1.68
HDPE29	2	HDPE	white	semi-opaque	0.64
HDPE30	2	HDPE	white	semi-opaque	1.15
LDPE01	4	LDPE	clear	semi-opaque	0.81
LDPE02	4	LDPE	clear	clear	0.59
LDPE03	4	LDPE	white	semi-opaque	6.66
LDPE04	4	LDPE	white	opaque	0.63
LDPE05	4	LDPE	clear	semi-opaque	0.79
LDPE06	4	LDPE	clear	semi-opaque	0.93
LDPE07	4	LDPE	clear	semi-opaque	0.91
LDPE08	4	LDPE	white	semi-opaque	1.99
LDPE09	4	LDPE	clear	semi-opaque	1.69
LDPE10	4	LDPE	clear	semi-opaque	2.10
LDPE11	4	LDPE	red	opaque	0.73
LDPE12	4	LDPE	white	opaque	12.74
LDPE13	4	LDPE	white	semi-opaque	1.53
LDPE14	4	LDPE	yellow	opaque	1.39
LDPE15	4	LDPE	white	semi-opaque	2.11
LDPE16	4	LDPE	clear	clear	1.12
LDPE17	4	LDPE	white	opaque	12.57
LDPE18	4	LDPE	clear	semi-opaque	1.10
LDPE19	4	LDPE	red	opaque	0.78
LDPE20	4	LDPE	clear	clear	0.98

Optics EXPRESS

Name	Recycling Code	Type	Color	Opaqueness	Thickness (mm)
LDPE21	4	LDPE	red	opaque	0.70
LDPE22	4	LDPE	white	opaque	0.71
LDPE23	4	LDPE	white	semi-opaque	6.43
LDPE24	4	LDPE	clear	semi-opaque	3.13
LDPE25	4	LDPE	red	opaque	0.69
LDPE26	4	LDPE	clear	semi-opaque	0.71
LDPE27	4	LDPE	clear	semi-opaque	0.86
LDPE28	4	LDPE	clear	semi-opaque	3.21
LDPE29	4	LDPE	red	opaque	0.74
LDPE30	4	LDPE	blue	opaque	1.24
PP01	5	PP	black	opaque	0.59
PP02	5	PP	clear	clear	0.63
PP03	5	PP	white	opaque	0.42
PP04	5	PP	clear	semi-opaque	0.59
PP05	5	PP	black	opaque	0.62
PP06	5	PP	white	opaque	0.50
PP07	5	PP	white	opaque	0.72
PP08	5	PP	black	opaque	0.52
PP09	5	PP	white	opaque	1.29
PP10	5	PP	white	opaque	0.60
PP11	5	PP	clear	semi-opaque	0.57
PP12	5	PP	white	opaque	0.65
PP13	5	PP	white	opaque	0.87
PP14	5	PP	clear	clear	0.49
PP15	5	PP	clear	semi-opaque	0.91
PP16	5	PP	clear	clear	0.49
PP17	5	PP	clear	clear	0.44
PP18	5	PP	clear	semi-opaque	0.81
PP19	5	PP	clear	clear	1.28
PP20	5	PP	clear	clear	0.96
PP21	5	PP	white	opaque	0.53
PP22	5	PP	white	opaque	0.64
PP23	5	PP	clear	clear	0.52
PP24	5	PP	green	opaque	1.10
PP25	5	PP	black	opaque	1.36
PP26	5	PP	clear	clear	0.72
PP27	5	PP	white	opaque	0.87
PP28	5	PP	blue	opaque	0.88
PP29	5	PP	clear	clear	0.78
PP30	5	PP	white	opaque	0.65
PS01	6	PS	white	opaque	0.33
PS02	6	PS	white	opaque	0.31

Optics EXPRESS

Name	Recycling Code	Type	Color	Opaqueness	Thickness (mm)
PS03	6	PS	white	opaque	0.33
PS04	6	PS	purple	opaque	0.57
PS05	6	PS	purple	opaque	0.52
PS06	6	PS	purple	opaque	0.55
PS07	6	PS	white	opaque	0.59
PS08	6	PS	white	opaque	0.54
PS09	6	PS	white	opaque	0.56
PS10	6	PS	clear	semi-opaque	0.33
PS11	6	PS	clear	semi-opaque	0.37
PS12	6	PS	clear	clear	0.26
PS13	6	PS	white	semi-opaque	0.52
PS14	6	PS	white	semi-opaque	0.40
PS15	6	PS	black	opaque	0.48
PS16	6	PS	white	opaque	0.31
PS17	6	PS	white	opaque	0.33
PS18	6	PS	clear	semi-opaque	0.41
PS19	6	PS	clear	semi-opaque	0.37
PS20	6	PS	clear	semi-opaque	0.20
PS21	6	PS	white	opaque	0.30
PS22	6	PS	black	opaque	0.33
PS23	6	PS	white	opaque	0.33
PS24	6	PS	white	opaque	0.32
PS25	6	PS	white	opaque	9.93
PS26	6	PS	clear	clear	0.20
PS27	6	PS	white	opaque	0.34
PS28	6	PS	black	opaque	0.34
PS29	6	PS	white	semi-opaque	0.54
PS30	6	PS	white	opaque	11.57

Funding

Richard Saltonstall Charitable Foundation; National Academies Keck Futures Initiative (NAKFI DBS13).

Disclosures

The authors declare that there are no conflicts of interest related to this article.

References

1. W. J. Shim, S. H. Hong, and S. E. Eo, "Identification methods in microplastic analysis: a review," Anal. Methods **9**(9), 1384–1391 (2017).
2. M. R. Jung, F. D. Horgen, S. V. Orski, V. Rodriguez C, K. L. Beers, G. H. Balazs, T. T. Jones, T. M. Work, K. C. Brignac, S.-J. Royer, K. D. Hyrenbach, B. A. Jensen, and J. M. Lynch, "Validation of ATR FT-IR to identify polymers of plastic marine debris, including those ingested by marine organisms," Mar. Pollut. Bull. **127**, 704–716 (2018).
3. J. Anzano, B. Bonilla, B. Montull-Ibor, and J. Casas-González, "Plastic identification and comparison by multivariate techniques with laser-induced breakdown spectroscopy," J. Appl. Polym. Sci. **121**(5), 2710–2716 (2011).

Optics EXPRESS

4. J. M. Anzano, I. B. Gornushkin, B. W. Smith, and J. D. Winefordner, "Laser-induced plasma spectroscopy for plastic identification," Polym. Eng. Sci. **40**(11), 2423–2429 (2000).
5. M. A. Gondal and M. N. Siddiqui, "Identification of different kinds of plastics using laser-induced breakdown spectroscopy for waste management," J. Environ. Sci. Health, Part A: Toxic/Hazard. Subst. Environ. Eng. **42**(13), 1989–1997 (2007).
6. H. Masoumi, S. Mohsen Safavi, and Z. Khani, "Identification and Classification of Plastic Resins using Near Infrared Reflectance Spectroscopy," World Acad. Sci. Eng. Technol. Int. J. Mech. Mechatron. Eng. **6**, 877–884 (2012).
7. V. Allen, J. H. Kalivas, and R. G. Rodriguez, "Post-Consumer Plastic Identification Using Raman Spectroscopy," Appl. Spectrosc. **53**(6), 672–681 (1999).
8. K. M. M. Shameem, K. S. Choudhari, A. Bankapur, S. D. Kulkarni, V. K. Unnikrishnan, S. D. George, V. B. Kartha, and C. Santhosh, "A hybrid LIBS–Raman system combined with chemometrics: an efficient tool for plastic identification and sorting," Anal. Bioanal. Chem. **409**(13), 3299–3308 (2017).
9. W. Becker, K. Sachsenheimer, and M. Klemenz, "Detection of Black Plastics in the Middle Infrared Spectrum (MIR) Using Photon Up-Conversion Technique for Polymer Recycling Purposes," Polymers **9**(12), 435 (2017).
10. T. K. Boyson, D. R. Rittman, T. G. Spence, M. E. Calzada, A. G. Kallapur, I. R. Petersen, K. Paul Kirkbride, D. S. Moore, and C. C. Harb, "Pulsed quantum cascade laser based hypertemporal real-time headspace measurements," Opt. Express **22**(9), 10519–10534 (2014).
11. R. F. Curl, F. Capasso, C. Gmachl, A. A. Kosterev, B. McManus, R. Lewicki, M. Pusharsky, G. Wysocki, and F. K. Tittel, "Quantum cascade lasers in chemical physics," Chem. Phys. Lett. **487**(1-3), 1–18 (2010).
12. A. Kosterev, G. Wysocki, Y. Bakhirkin, S. So, R. Lewicki, M. Fraser, F. Tittel, and R. F. Curl, "Application of quantum cascade lasers to trace gas analysis," Appl. Phys. B **90**(2), 165–176 (2008).
13. C. C. Harb, T. K. Boyson, A. G. Kallapur, I. R. Petersen, M. E. Calzada, T. G. Spence, K. P. Kirkbride, and D. S. Moore, "Pulsed quantum cascade laser-based CRDS substance detection: real-time detection of TNT," Opt. Express **20**(14), 15489–15502 (2012).
14. M. Brandstetter, L. Volgger, A. Genner, C. Jungbauer, and B. Lendl, "Direct determination of glucose, lactate and triglycerides in blood serum by a tunable quantum cascade laser-based mid-IR sensor," Appl. Phys. B **110**(2), 233–239 (2013).
15. S. Liakat, K. A. Bors, L. Xu, C. M. Woods, J. Doyle, and C. F. Gmachl, "Noninvasive in vivo glucose sensing on human subjects using mid-infrared light," Biomed. Opt. Express **5**(7), 2397–2404 (2014).
16. H. von Lilienfeld-Toal, M. Weidenmüller, A. Xhelaj, and W. Mäntele, "A novel approach to non-invasive glucose measurement by mid-infrared spectroscopy: The combination of quantum cascade lasers (QCL) and photoacoustic detection," Vib. Spectrosc. **38**(1-2), 209–215 (2005).
17. A. Kassouf, J. Maalouly, D. N. Rutledge, H. Chebib, and V. Ducruet, "Rapid discrimination of plastic packaging materials using MIR spectroscopy coupled with independent components analysis (ICA)," Waste Manage. (Oxford, U. K.) **34**(11), 2131–2138 (2014).
18. O. Rozenstein, E. Puckrin, and J. Adamowski, "Development of a new approach based on midwave infrared spectroscopy for post-consumer black plastic waste sorting in the recycling industry," Waste Manage. (Oxford, U. K.) **68**, 38–44 (2017).
19. D. Saviello, L. Toniolo, S. Goidanich, and F. Casadio, "Non-invasive identification of plastic materials in museum collections with portable FTIR reflectance spectroscopy: Reference database and practical applications," Microchem. J. **124**, 868–877 (2016).
20. K. A. Whittaker, J. Keaveney, I. G. Hughes, and C. S. Adams, "Hilbert transform: Applications to atomic spectra," Phys. Rev. A **91**(3), 032513 (2015).
21. M. Boulet-Audet, T. Buffeteau, S. Boudreault, N. Daugey, and M. Pézolet, "Quantitative Determination of Band Distortions in Diamond Attenuated Total Reflectance Infrared Spectra," J. Phys. Chem. B **114**(24), 8255–8261 (2010).
22. M. Picollo, G. Bartolozzi, C. Cucci, M. Galeotti, V. Marchiafava, and B. Pizzo, "Comparative Study of Fourier Transform Infrared Spectroscopy in Transmission, Attenuated Total Reflection, and Total Reflection Modes for the Analysis of Plastics in the Cultural Heritage Field," Appl. Spectrosc. **68**(4), 389–397 (2014).
23. S. Krimm, *Infrared Spectra of High Polymers. In Fortschritte Der Hochpolymeren-Forschung* (Springer, Berlin, Heidelberg, 1960).
24. G. Wysocki, R. F. Curl, F. K. Tittel, R. Maulini, J. M. Bulliard, and J. Faist, "Widely tunable mode-hop free external cavity quantum cascade laser for high resolution spectroscopic applications," Appl. Phys. B **81**(6), 769–777 (2005).
25. B. G. Lee, M. A. Belkin, R. Audet, J. MacArthur, L. Diehl, C. Pflügl, F. Capasso, D. C. Oakley, D. Chapman, A. Napoleone, D. Bour, S. Corzine, G. Höfler, and J. Faist, "Widely tunable single-mode quantum cascade laser source for mid-infrared spectroscopy," Appl. Phys. Lett. **91**(23), 231101 (2007).
26. L. Dong, V. Spagnolo, R. Lewicki, and F. K. Tittel, "Ppb-level detection of nitric oxide using an external cavity quantum cascade laser based QEPAS sensor," Opt. Express **19**(24), 24037–24045 (2011).
27. Z. Li, C. Shi, and W. Ren, "Mid-infrared multimode fiber-coupled quantum cascade laser for off-beam quartz-enhanced photoacoustic detection," Opt. Lett. **41**(17), 4095–4098 (2016).
28. V. Spagnolo, P. Patimisco, S. Borri, G. Scamarcio, B. E. Bernacki, and J. Kriesel, "Mid-infrared fiber-coupled QCL-QEPAS sensor," Appl. Phys. B **112**(1), 25–33 (2013).
29. J. Brandon, M. Goldstein, and M. D. Ohman, "Long-term aging and degradation of microplastic particles: Comparing in situ oceanic and experimental weathering patterns," Mar. Pollut. Bull. **110**(1), 299–308 (2016).